

Estimation of Stiffness Derivative of an Ogive for Specific Heat Ratio 1.666

Aysha Shabana¹, Renita Sharon Monis², Asha Crasta³, and S.A.Khan^{4*}

¹ Research Scholar, Mathematics Dept., M.I.T.E, Moodabidri, and Assistant Professor, SCEM, Mangaluru, Karnataka, India

² Research Scholar, Mathematics Dept., M.I.T.E, Moodabidri and Assistant Professor, SMVITM, Bantakal, Karnataka, India

³ Associate Professor, Mathematics Department, M.I.T.E, Moodabidri, Karnataka, India

⁴ Professor, Department of Mechanical Engineering, Faculty of Engineering, IIUM, Gombak Campus, Kuala Lumpur, Malaysia.

Article Info

Volume 81

Page Number: 5091 - 5100

Publication Issue:

November-December 2019

Abstract:

This paper focusses attention on studying the effect of the flow medium on the aerodynamic characteristics of the ogive at significant inertia levels. Accordingly, the hypersonic similitude is used to find an analytical expression to evaluate the pressure dissemination on the exterior of the ogive and hence, finally to get the stiffness derivatives for Mach quantities from $M = 5$ to 15, and the streamwise directions in the range from 100 to 250. This study considers two values of the $\lambda = 5$, and 10 are for the ogival shape of the nose. The γ value considered is 1.666. Using this value of the specific heat ratio the expression for rigidity derived for an ogive through the assumption that the gas is in-viscid and ideal, the indication is semi-steady, and the front nose approach of the ogive is to such an extent that the inertia level behind the shock $M_2 \geq 2.5$. The consequences designate that with the rise in the Mach number since $M = 5$ to $M = 15$, initially the magnitude of the stiffness derivative and later with superfluous rise in the Mach (M), it befits self-regulating of inertia level and Mach independence principle has revisited. When the $\lambda = 10$, there is a swing of the midpoint of force towards the leading edge.

Article History

Article Received: 5 March 2019

Revised: 18 May 2019

Accepted: 24 September 2019

Publication: 24 December 2019

I. INTRODUCTION:

The knowledge of firmness derives in the arena due to the proportion of terrain, and the rate of the angle of attack is of prime importance. The prediction of their numerical values is of utmost importance. During the flight, whenever there is an increase in the angle of attack, this would result in a pitch up moment. Under these circumstances, to bring back the aerodynamic object to its equilibrium position, the stiffness derivative shows a significant part. The magnitude of the stiffness is dependent on the center of gravity of the object, the

stress spreading on the apparent, and the position of resultant center of stress, which decides static margin in case of the aerodynamic vehicle. The present work assesses strength subsidiaries in terrain for non-thin axis-symmetric Ogives wavering in hypersonic stream. At hypersonic speediness, the "front pine cones" regularly have a low L/D ratio; usually, the nose is blunt and obtuse. The tenacity behind such an operation is the issue of streamlined bodies, the extraordinary temperature created at the nose, which is significant that may lead to ablation of the surface material. In spitefulness of the statement that the contemporary work

isn't for streamlined forms with separate out steps when a postulate is generated aimed at the ogives with a high-pitched front nose, it would now be competent to be extended out to reenter earth gradually downcast to connection the ambient atmosphere.

It is sincerely enthralling to proceed annotation of that the exploration of high Mach tributaries, which has restricted itself for the frames with high L/D ratio, ought to accomplish a phase of the bodies with low L/D ratio with non-aerodynamic contours and universally line of attack torrents, talented and underscored expansion of creative imminent hypersonic outlines.

Ghosh (1977) constructed up alternative large Mach similitude with the devoted arc shock and Mach value just after the shock wave actuality extranotable > 2.5. This comparison is considerable for the upwind external of aero-foil with mammoth stream circumvention. Their effort further stretched out to swaying with curved wedges by Crasta and Khan to figure and rationalized endowings small holdings, both Supersonic ($M < 5$) Ghosh (1984) and

Hypersonic streams ($M > 5$) Asha Crasta et al. (2014).

The enormous rerouting comparability of earlier research has been overextended by Ghosh (1984) to axisymmetric figures with appended tremors. The likeness of extra cylinder movement, which has essential evenness that have been transformed of a wedge corpulent the along with the flow with a hinge, that comparable upset of free liquid section Ghosh (1977) yields a pivotally conical-annular interplanetary. He further showed that the torrent bygone a pinecone/semi funnel seems to be comparative to a container drive in conical-annular cosmos that was recognized as a level of the similitude. Despite the statement that Ghosh (1984) gives comparability for cones, he contributes an answer dependent on likeness for a cone as it were. The arrangement shows an even thickness shock film. Henceforth the steady thickness type of the unstable Bernoulli's condition is utilized to discover weight on the conduit exterior. The outcomes are becoming useful for high-speed flow for perfect gas over variable conduits of various inertia levels & flow deflection angles.

II. ANALYSIS

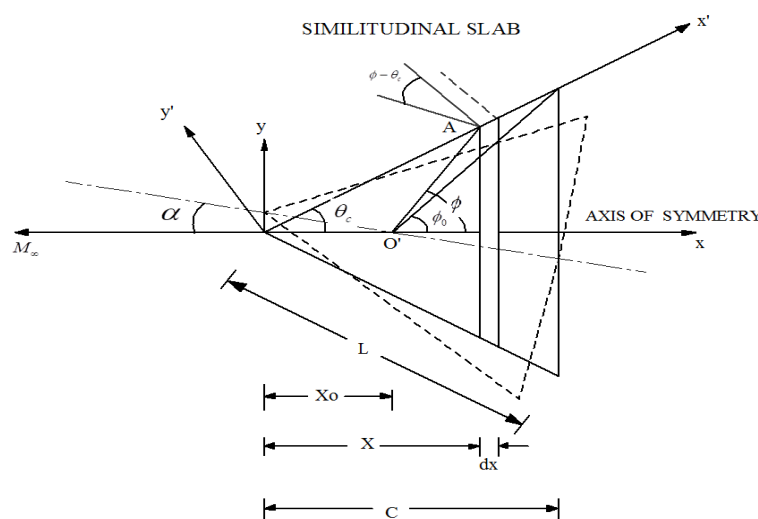


Figure 1: Cone Geometry

With Fig. 1 we have

$$\tan \phi = \frac{x \tan \theta}{(x - x_0)} ; \tan \phi_0 = \frac{c \tan \theta}{(c - x_0)}$$

Everywhere ϕ is the slant shaped by A at O' with x-axis, for the diverse position at A, ϕ fluctuates between π to ϕ_c ,

$\theta_c + \lambda$ is the half-angle of the ogive, and c being the dominant chord length?

The demarcation of the Rigidity measurements symbolized by C_{m_α} is

$$C_{m_\alpha} = \left[\frac{\partial M}{\partial \alpha} \right]_{\alpha, q \rightarrow 0} \frac{1}{\frac{1}{2} P_\infty U_\infty^2 S_b c}$$

Here S_b = base space of ogive = $\pi (c \tan \theta_c)^2$,
 c = triad size of ogive.

After simplification we get, the following equation

Equation of compression quotient of a fixed cone if a shock is devoted to the nose, is

$$\frac{P_{bo}}{P_\infty} = 1 + \gamma M_{po}^2 \left(1 + \frac{1}{4} \varepsilon \right) \quad (1)$$

Everywhere the concreteness quotient is

$$\varepsilon = \frac{2 + (\gamma - 1) M_{po}^2}{2 + (\gamma + 1) M_{po}^2} \quad (2)$$

M_{po} = piston inertia quantity of the corresponding motion of the piston, working in a conical-annular space, P_{bo} is the stress on frame exterior at prevalence are zero.

$$M_{po} = M_\infty \sin \theta_c$$

Everywhere θ_c = flow deflection angle?

Hence

$$\frac{dP_{bo}}{dM_{po}} = 2\gamma P_\infty M_{po} \left[1 + \frac{1}{4} \left(\varepsilon + \frac{1}{2} M_{po} \cdot \frac{d\varepsilon}{dM_{po}} \right) \right] \quad (3)$$

Where

$$\frac{d\varepsilon}{dM_{po}} = \frac{-8M_{po}}{N^2} + \lambda' f \left\{ \frac{8K(3(\gamma + 1)K^2 - 2)}{N^3} \right\} \quad (4)$$

$$\text{And } N = [2 + (\gamma + 1)M_{po}^2]$$

On resolving (3), we have

$$\frac{dP_{bo}}{dM_{po}} = 2\gamma P_\infty M_{po} \left[(a_1 + \lambda' a_2) - \frac{2a_2 \lambda' h \tan \phi}{\tan \phi - \tan \theta_c} \right] \quad (5)$$

Everywhere $h = \frac{x_0}{c}$,

$$\lambda' = \frac{\lambda}{\tan \theta_c},$$

$$a_1 = 1 + \frac{\varepsilon}{4} - \frac{K^2}{N^2}$$

$$a_2 = 1 + \frac{\varepsilon}{4} - \frac{K^2(N+8)}{N^3}$$

Utilizing the expressions obtained as above are used to evaluate the magnitude of the stability derivatives,

$$C_{m_q} = [C_{m_q}]_{cone} + \frac{\lambda' a_2}{15(1+n^2)} \left[h^4 \{5(2n^2 - 3n^4 - 1) - 4h(3n^2 - 6n^4 - 1)\} + (1-h) \{H(9H + (2n^2 - 3H)h + 2(2H + 3n^2)h^2 + 12n^2h^3) - n^4h^2(1 + 3h - 24h^2)\} \right]$$

Where

$$[C_{m_q}]_{cone} = (D/2) \left[h^4(2n^2 - 3n^4 - 1) - (1-h) \{H(3H + h(H + 2n^2) + 2h^2n^2) + n^4h^2(1 + 3h)\} \right]$$

$$D = \frac{2}{3(1+n^2)} \left[1 + \frac{1}{4} \left(\varepsilon + \frac{1}{2} K \frac{d\varepsilon}{dM_{po}} \right) \right] \quad (7)$$

$$H = (1 - h + n^2)$$

$$n = \tan \theta_c$$

Outcomes are computed for an extensive collection of angles of incidence, the inertia level M, and the ogive shapes are discussed.

III. RESULTS AND DISCUSSIONS

This primary focus of the study is to find influence of the specific heat ratio, the level of inertia, and the angles of incidence with the variations in the hinge positions.

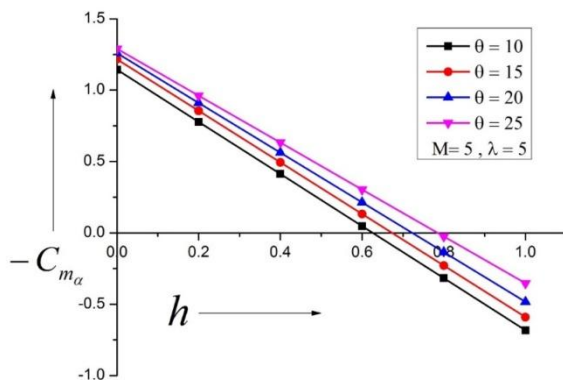


Fig. 1 Variant of stiffness derived Vs. h, Mach M = 5

Fig. 1 shows the toughness derived variations for different hinge positions from $h = 0$ to 1. The stiffness derivative has a similar trend for the complete choice of the inertia levels and the stream deflection angle from 10° to 25° . Results show that it starts with the highest value and decreases progressively crosses the point of the center of pressure and then continues to decrease till $h = 1$. While the stream drift is increased from 10° to 15° , 15° to 20° , and 20° to 25° for a fixed Mach $M = 5$ and the ogive shape where $\lambda = 5$, there is a maximum increase of 19% and a decrease of 27%. It is also seen that near the center of pressure, this increase is maximum and becomes 176%. For the next range of θ from 15 to 20 degrees, the increase marginal for the positions very closed to the nose; however, right near the epicenter of stress, it is 62%. For the locations beyond the center of pressure, the enhancement in the magnitude is 42%. For the highest range of the θ from 20 to 25 degrees, the gain for the 40 % of the nose is up to 12%, near the center of pressure, it is around 41 %, and beyond the center of pressure

on the negative side, it is 82 %. From the results, we observe a considerable rise in the toughness spinoffs for all the positions of the hinge h . The situation of the epicenter of stress is anxious; there is a continuous shift towards the trailing edge, which will be very handy as far as the stability of the aerospace vehicle. Due to this shift in the center of pressure, there will be a considerable increase in the moment arm and will result in a considerable increase in the nose-down moment to bring the aerospace vehicle to its equilibrium position once it is disturbed from its equilibrium position.

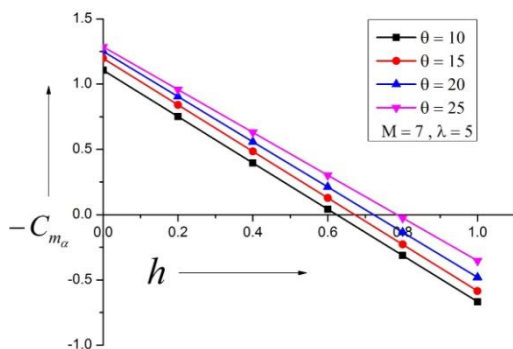


Fig. 2 Variant of stiffness derived Vs. h , Mach $M = 7$

Figure 2 displays variations in stability derivative for a slightly large Mach number for $M = 7$. This upsurge in the Mach number effects in a marginal reduction in the stability derivatives as it is seen while scanning the literature that indicates that there is an advanced reduction in the stability byproducts in view of the rise in M which results in a totally different pressure distribution on the external of the ogive. The flow pattern will be totally dissimilar from that of the cone surface. We know that for cone, there will be a robust slanting shock that will be located at the nose of the cone. This oblique shock will result in a pressure jump after the shock, which indicates the strength of the oblique shock. This strength of the oblique shock will be different at diverse Mach & the flow deflections. The

remaining pattern remains the same as discussed above.

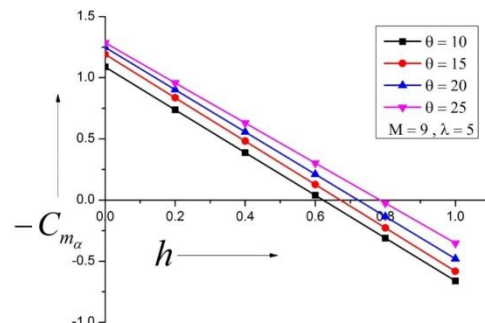


Fig. 3 Variant of stiffness derived Vs. h , Mach $M = 9$

Fig. 3 presents the variant of the stability derivatives Vs. the hinge point for an increased inertia from $M = 7$ to $M = 9$. As discussed earlier, due to this upsurge in Mach, the shock power will be increased, leading to changed forces spreading on the ogive exterior and hence, the decreased values of the stability derivatives. The center of stress lies from $h = 0.62$ to 0.8 , and this shift is linear all along with the angles. Outcomes show a marginal increase in the percentage change on the positive side, whereas beyond the epicenter of stress on the negative range is identical. The results indicate that the extreme upsurge is 231 %, which is maximum at $h = 0.6$ for $\lambda = 5$, and the flow deflection angle increase from 10 to 15 degrees. For other flow deflection angle $\theta = 20$ and 25 degrees, this growth in the stability derivative remains in the kind from 45 to 65 percent. Since the Mach number for the present case is $M = 9$, which seems to be very closed to inertia when the Mach number liberation belief prevails. Any further growth in the inertia level will not produce any variation in the stability derivatives.

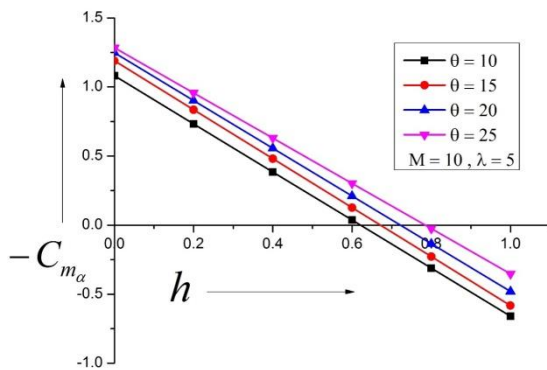


Fig. 4 Variant of stiffness derived Vs. h , Mach $M = 10$

Results for Mach $M = 10$ are shown in Fig. 4. Due to the growth in the inertia level, nearby is a further increase in stiffness stability derivative at hinge location of $h = 0.6$ by nearly ten percent. When $\theta = 20^\circ$ and 25° , there is a marginal increase in the value of $C_{m_{\alpha}}$. Locations of the center of pressure also remained the same. The results at this Mach number also display the same trend, as existed seen in the earlier cases.

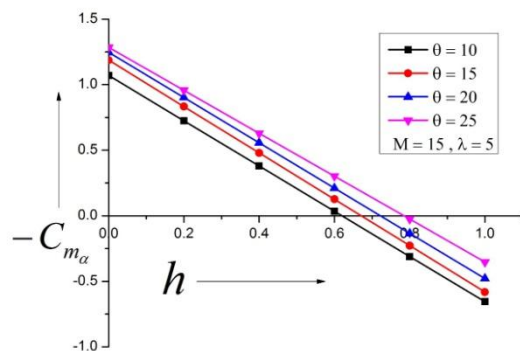


Fig. 5 Variant of stiffness derived Vs. h , Mach $M = 15$

Figure 5 displays outcomes of stiffness derivatives for $M = 15$, which is the highest inertia level considered. It is found, the growth in the inertia level results in a further increase in the percentage enhancement of the stiffness

derivatives at $h = 0.6$, which is 264 %. However, for $\theta = 20^\circ$ and 25° , the percentage increase remains nearly the same as was seen for lower Mach numbers. As far as the center of pressure location is concerned, there is a marginal shift towards the leading edge. Except for these changes, remaining parameters show similar trends, as was comprehended at Mach $M = 5$ to 10.

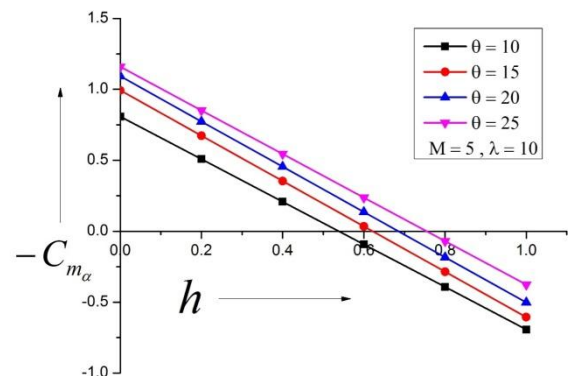


Fig. 6 Variant of stiffness derived Vs. h , Mach $M = 5$

Figure 6 displays the consequences of the toughness spinoffs for increase ogive arc for the lowest Mach number $M = 5$ for different pivot positions. The percentage escalation in the stiffness derived is in the sort from 22.8, 32.4, 69.7, -136.7, -27, and -12 while the flow ricochet slant θ is augmented from 10° to 15° . The % centage growth in the toughness imitative is in the assortment from 10, 15, 28.7, 301, -36, and -17 while the stream ricochet θ is amplified from 15° to 20° . The percentage upturn in the stiffness derived ranges from 6, 10, 19.8, 74.9, -62, and -25 for the drift ricochet θ is increased 20° to 25° . It is observed that the positions of the center of pressure for different $\theta = 10^\circ, 15^\circ, 20^\circ$, and 25° , the location of epicenter of stress is at $h = 0.52$, for $\theta = 15^\circ$ the site of epicenter of stress has relocated in the route of the straggling verge, is located at $h = 0.62$, for $\theta = 20^\circ$ the of epicenter of stress has shifted further in the course of the behind edge

and is established to be at $h = 0.69$, for $\theta = 25^\circ$ it has further advanced and shifted towards the straggling edge and is located at $h = 0.76$. The reasons for this trend may be the ogival arc, which has changed the geometry of the nose. Due to the increased arc radius, it will modify the flow field completely on the surface of the ogive. The increased radius has modified the flow field in such a way that the epicenter of stress stimulated on the way to the leading end.

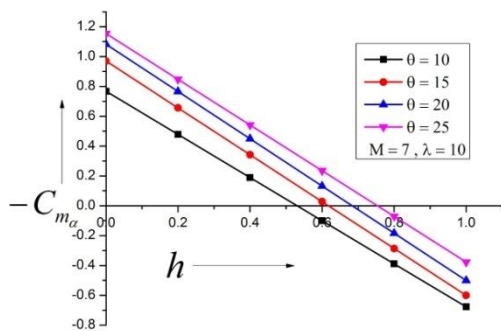


Fig. 7 Variant of toughness derived Vs. h , Mach $M = 7$

The same outcomes are seen in figure 7 when Mach is augmented from $M = 5$ to 7. The percentage intensification in the stiffness derived remains from 26.5, 37.3, 80.9, -128.2, -26, and -11.5 while the streamricochet angle θ is increased 10° to 15° . The percentage growth in the toughness derived is in the variety from 11, 17, 32, 371, -36, and -17 when the flow deflection angle θ is augmented 15° to 20° . The percentage growth in the stiffness derived remained from 7, 11, 21, 77, -61.7, and -25 while the streamricochet angle θ is augmented from 20° to 25° . The center of pressure remained at $h = 0.52$ to $h = 0.77$. Rest of the pattern remained the same.

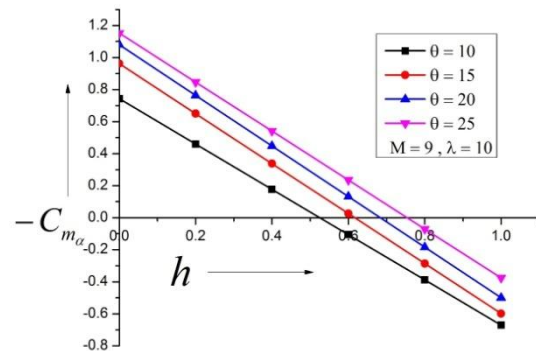


Fig. 8 Variant of stiffness derived Vs. h , Mach $M = 9$

Results at Mach number $M = 9$ for $\lambda = 10$ be presently displayed in figure 8 for various streamricochet slants. The percentage growth in the stiffness derived ranges from 29, 41, 90, -124.6, -26.3, and -10.9 while the flow ricochet viewpoint θ is augmented 10° to 15° . The percentage growth in the toughness derived varied in the range from 12.2, 17.5, 32.5, 408.9, -36, and -16.4 while the streamricochet slant θ is augmented from 15° to 20° . The percentage growth in the stiffness derived ranges from 7, 11, 20.9, 78.5, -61.7, and -24.7 while the flow rebound viewpoint θ is augmented 20° to 25° . As seen earlier with the growth in the streamricochet angle $\theta = 10^\circ$ to 25° , this would lead to enhancement in the planform area of the ogive. This increased surface area will change the pressure pattern along the length of the ogive. The center of pressure also will change, with increasing θ it will shift towards the downstream. The shift of the center of pressure with an increase in θ will result in an increased value of the stability derivatives as the center of gravity is fixed; it will not change.

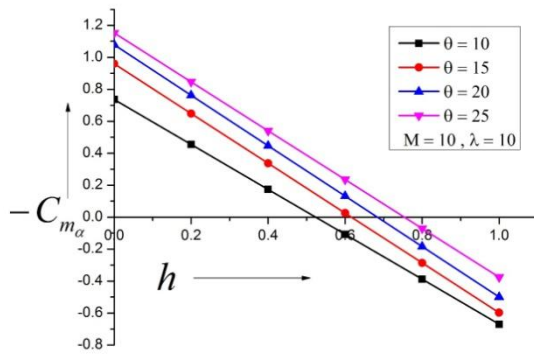


Fig. 9 Variant of stiffness derived Vs. h , Mach $M = 10$

Results at Mach number $M = 10$ for $\lambda = 10$ are displayed in figure 9 for various flow deflection angles. The percentage rise in the stiffness derived ranges from 30.4, 42.5, 93.6, -124.6, -26.3, and -10.7 while the flow deflection angle θ is augmented from 10° to 15° . The percentage proliferation in the stiffness derived ranges from 12.4, 17.7, 32.8, 419.5, -35.7, and -16.4 when viewpoint θ is improved 15° to 20° . The percentage growth in the stiffness derived ranges from 6.8, 11, 21, 78.7, -61.7, and -24.7 when angle θ is amplified 20° to 25° . This increased surface area will change the pressure pattern along the length of the ogive. The center of pressure also will change, with increasing θ it will shift towards the downstream. The shift of the center of pressure with an increase in θ will result in the improved worth of the stability derivatives as the center of gravity is fixed; it will not change.

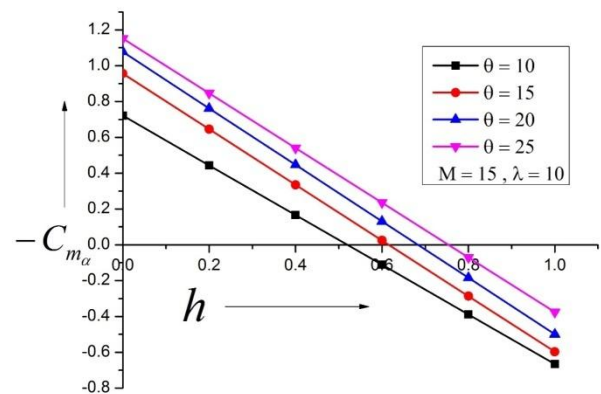


Fig. 10 Variant of stiffness derived Vs. h , Mach $M = 15$

Outcomes at $M = 15$ for $\lambda = 10$ are displayed in figure 10 for various flow deflection angles. The percentage rise in the stiffness derived ranges from 32.6, 45.5, 101.6, -121.8, -26.4, and -10.4 while the flow deflection angle θ is amplified from 10° to 15° . The percentage rise in the toughness derived ranges from 12.6, 18, 33, 440, -35.7, and -16.3 once angle θ is increased 15° to 20° . The percentage upsurge in the stiffness derived ranges from 7, 11, 21, 79, -61.7, and -24.7 as soon as the flow deflection angle θ is amplified 20° to 25° . As seen earlier by way of the growth in the stream deflection point of view $\theta = 10^\circ$ to 25° , this would lead to enhancement in the planform area of the ogive. This increased surface area will change the pressure pattern along the length of the ogive. The center of pressure also will change, with increasing θ it will shift towards the downstream. The shift of the center of pressure with an increase in θ will result in the increased value of the stability derivatives as the center of gravity is fixed; it will not change.

IV. Conclusions:

Recognized on the below pondering, we cement the succeeding decisions:

- The stiffness declines with the rise of inertia level, and for inertia level, $M = 10$ and beyond, nearby, the present is no modification in the magnitude of the stability derivative leading to the Mach unconventional opinion.
- There is an enlightened growth in the firmness derived from the ogive due to the growth in the streamricochet slant to the growth in the surface space of the ogive. Also, it is seen that by a proliferation in the flow deflection viewpoint, there is an incessant swing in the center of pressure in the direction of the downstream.
- It is seen that when the $\lambda = 10$, there is a move in the epicenter of pressure towards the foremost edge. This shift will change the stability scenario of the ogive forebody.

References

1. Ghosh, K., 1977. A New Similitude for Aerofoils in Hypersonic Flow. Proceedings of the 6th Canadian Congress of Applied Mechanics, Vancouver, Canada, May 29-June 3, pp. 685-686.
2. Ghosh, K., 1984. Hypersonic large deflection similitude for oscillating delta wings. The Aeronautical Journal, pp. 357-361.
3. S. A. Khan and Asha Crasta, "Oscillating Supersonic Delta wing with curved Leading Edges," International Journal of Advanced Studies in Contemporary Mathematics, Volume 20, No. 3, pp. 359-372, July 2010, ISSN: 12293067.
4. Asha Crasta, Pavitra S., S. A. Khan, "Estimation of Pressure Distribution on A Delta Wing with Curved Leading Edges in Hypersonic/Supersonic Flow", International Journal of Energy, Environment, and Economics published by NOVA Science Publishers, Volume 24, Issue 1, pp. 67-73, 2016 (ISSN: 1054-853X).
5. S. Pavithra, S. Lavanya, S. A. Khan, and Asha Crasta, "Estimation of Aerodynamic Derivatives in Pitch of a Wedge in Hypersonic Flow", Indian Journal of Science and Technology, Volume 9, Issue 34, pp. 1-4, September 2016, ISSN (Print): 0974-6846, ISSN (online): 0974-5645, DOI: 10.17485/v9i34/100958.
6. S. Pavitra, Musavir Bashir, S. Lavanya, and S. A. Khan, "Estimation of Stability Derivatives in Pitch for an oscillating 2-D Wedge in Supersonic Flow", International Journal of Advances and Applications in Fluid Mechanics, Volume 19, Issue 4, pp. 873-882, 2016, ISSN: 0973-4686, DOI: <http://dx.doi.org/10.17654/FM019040873>.
7. S. A. Khan, and Mohammad Asad Ullah, "Estimation of Stability Derivatives in Pitch for an Oscillating Wedge in Hypersonic Flow," IOP Publishing House, IOP Conf. Series: Materials Science and Engineering 184, pp. 1-7, April 2017 012003 DOI: 10.1088/1757-899X/184/1/012003.
8. Musavir Bashir, S. A. Khan, Leelanadh Udayagiri, and Asim Noor, "Dynamic Stability of Unguided Projectile with 6-DOF Trajectory Modelling," 2017 2nd International Conference for Convergence in Technology (I2CT), India, December 2017, published by IEEE Explorer USA, pp. 1121-1125, DOI: 10.1109/I2CT.2017.8226302, URL: <http://ieeexplore.ieee.org/stamp/stamp.jsp?tp=&arnumber=8226800&isnumber=8226083>.
9. Pavitra S, Lavanya S., and S. A. Khan, "Stability derivatives of oscillating wedges in viscous hypersonic flow," IOP Publishing House, IOP Conf. Series: Materials Science and Engineering 370, pp. 1-9, May 2018, 012051, DOI: 10.1088/1757 899X /370 /1/ 012051.
10. Aysha Shabana, Renita Sharon Monis, Asha Crasta, and S. A. Khan, "Computation of Stability Derivatives of an oscillating cone for specific heat ratio 1.66", IOP Publishing House, IOP Conf. Series: Materials Science and Engineering 370, pp. 1-11, May 2018, 012059 DOI: 10.1088/1757 899X /370 /1/ 012059.
11. Aysha Shabana, Renita Sharon Monis, Asha Crasta, and S. A. Khan, "Estimation of Stability Derivatives in Newtonian Limit for Oscillating Cone," IOP Publishing House, IOP Conf. Series:

- Materials Science and Engineering 370, pp. 1-10, May 2018, 012061 DOI: 10.1088/1757 899X /370 /1/ 012061.
12. Ayesha Shabana, Renita Sharon Monis, Asha Crasta, and S. A. Khan, "The Computation of Stiffness Derivative for an Ogive in Hypersonic Flow", International Journal of Mechanical and Production Engineering Research and Development (IJMPERED), Vol. 8, Issue 5, pp. 173-184, June, 2018, ISSN (online): 2249-8001, ISSN (Print): 2249-6890.
 13. Renita Sharon Monis, Asha Crasta, and S. A. Khan, "Evaluation of Stiffness Derivative for a Delta Wing with Straight Leading Edges in Unsteady Flow," International Journal of Engineering and Advanced Technology (IJEAT), ISSN: 2249-8958, Volume 8, Issue 3S, pp. 754-762, February 2019.
 14. Sher Afghan Khan, Abdul Aabid, Ahamed Saleel C, "CFD Simulation with Analytical and Theoretical Validation of Different Flow Parameters for the Wedge at Supersonic Mach Number", International Journal of Mechanical & Mechatronics Engineering IJMME-IJENS, Vol. 19, No. 01, pp. 170-177, February, 2019, ISSN: 2077-124X (Online) , ISSN: 2227-2771 (Print), ISSN: 2227-2771 (Print).
 15. Renita Sharon Monis, Aysha Shabana, Asha Crasta, and S. A. Khan, "Effect of Sweep Angle and a Half Sine Wave on Roll Damping Derivative of a Delta Wing" International Journal of Recent Technology and Engineering (IJRTE) ISSN: 2277-3878, Volume 8, Issue 2S3, pp. 984-989, August 2019, DOI : 10.35940/ijrte.B1184.0782S319.
 16. Aysha Shabana, Renita Sharon Monis, Asha Crasta, Sher Afghan Khan, "Damping Derivative Evaluation in Pitch for an Ogive at High Mach Numbers", International Journal of Innovative Technology and Exploring Engineering (IJITEE), Volume-8, Issue-12, pp. 1307-1317, October 2019, ISSN: 2278-3075, DOI: 10.35940/ijitee.L3918.1081219.
 17. Renita Sharon Monis, Asha Crasta and S. A. Khan, "Estimation of Damping Derivatives for Delta Wings in Hypersonic Flow for Straight Leading Edge," International Journal of Mechanical and Production Engineering Research and Development (IJMPERD), pp. 255-264, October 2019, DOI : 10.24247/ijmperdoct201922.
 18. Renita Sharon Monis, Asha Crasta, Mohammed Faheem, and S. A. Khan, "Analysis of Damping Derivatives for Delta Wings in Hypersonic Flow for Curved Leading Edges with Full Sine Wave," International Journal of Engineering and Advanced Technology (IJEAT), Volume 9 Issue-1, pp. 5457-5466, October 2019, ISSN: 2249 – 8958, DOI: 10.35940/ijeat.A3086.109119.